Tellurium retention by containment spray system

(article starts on next page)

Tellurium retention by containment spray system

Teemu Kärkelä [a,*], Anna-Elina Pasi [b], Fredrik Espegren [b], Tuomo Sevón [a], Unto Tapper [a], Christian Ekberg [b]

[a] VTT Technical Research Centre of Finland Ltd, P.O. Box 1000, FI-02044 VTT, Espoo, Finland
[b] Chalmers University of Technology, Kemivägen 4, SE-412 96 Gothenburg, Sweden

ARTICLE INFO

ABSTRACT

A containment spray system is used to mitigate the source term from the containment building to the environment as part of the severe accident management actions. Tellurium is one of the volatile fission products and many of the tellurium isotopes decay into iodine, which causes a threat to the public due to its radiotoxicity and build-up in the thyroid gland. The removal efficiency of the containment spray system model against tellurium species formed under severe accident conditions was investigated with experiments and MELCOR simulations. The results indicated efficient removal of tellurium aerosols in the air atmosphere, whereas a decrease in the efficiency was observed in the nitrogen atmosphere. Gaseous tellurium species were not formed in significant amounts during the experiments and therefore, the removal efficiency due to different spray chemistry conditions could not be accurately analysed. However, the alkaline chemicals used in the spray solution seemed to form airborne particles, increasing the overall aerosol transport in the process independently of CsI or Te aerosol transport.

1. Introduction

In a severe nuclear power plant (NPP) accident where the core integrity has been lost, one of the main concerns is to minimize the release of radioactive fission products (FP) to the environment. As part of the severe accident management (SAM) actions, various engineered safety systems have been developed. These systems respond to unlikely situations during accident progression and aim to minimize the consequences of an accident. One of these SAM actions is the operation of a containment spray system (CSS). The CSS has been designed for several accident management purposes, including containment pressure suppression, heat removal, sump chemistry control and FP scavenging from the containment atmosphere (Neeb, 2011).

Tellurium is one of the volatile FPs and it is released in significant amounts during a severe accident. Moreover, many of the released tellurium isotopes decay into iodine and therefore, have an effect on the iodine source term. It is estimated that around 1400 PBq of tellurium, mostly ^{132}Te (1150 PBq), was released into the environment during the Chernobyl accident. In comparison to the release of ^{131}I from the Chernobyl accident, 1760 PBq, the tellurium releases are of the same magnitude and therefore should be considered significant. The Fukushima accident resulted in releases

of around 180 PBq and 150 PBq ^{132}Te and ^{131}I releases, respectively (UNSCEAR, 2008; Steinhauser et al., 2014).

The release of tellurium from a fuel assembly in the early stage of an accident is delayed by the zirconium cladding. However, in the case of sufficiently high temperature (ca. 2620 K) (Pontillon and Ducros, 2010) or once the cladding becomes sufficiently oxidized, tellurium species are released into the reactor coolant system (RCS), subsequently into the containment building and finally into the environment (Boer and Cordfunke, 1997). The speciation of the released tellurium is highly dependent on the prevailing conditions in the RCS and the containment building (Espegren et al., 2020; McFarlane, 1996; Jones et al., 2015; Sangiorgi et al., 2015). The main tellurium species entering the containment include different tellurium oxides, elemental tellurium, tin telluride and caesium tellurides (McFarlane, 1996).

The release and transport of tellurium together with other FPs from the core and the behaviour in the containment has been investigated as part of the PHÉBUS experimental programme (Laurie et al., 2013). It was found that the majority of the released tellurium was associated with the fission product aerosol particles. The tellurium-bearing species were found to be removed from the containment atmosphere mostly by gravitational settling and partly by diffusiophoresis (Laurie et al., 2013). Furthermore, the condensed and deposited tellurium species on the surfaces were washed to the vessel's bottom and the sump. Although research has been conducted in terms of tellurium release and transport

behavior, the effectiveness of CSS specifically on the airborne tellurium removal from the containment atmosphere is still unclear.

In this work, the objective was to investigate the tellurium species formed in oxidizing and inert atmospheres and their removal from the atmosphere using water and alkaline droplets, simulating the spray chemistry used in the SAM actions. To proceed from a single component system towards more complex conditions, airborne caesium iodide particles were fed together with tellurium to examine the impact on tellurium removal. Caesium iodide is expected to be present in the containment atmosphere together with tellurium species at the same time (OECD/NEA, 2009). Another objective was to simulate the experiments using the MELCOR severe accident analysis code to verify the experimental removal efficiency results and to identify possible needs for code development. To summarize, this work aims to provide information about the efficiency of the containment spray system on tellurium removal and produce data that can be used for severe accident code improvement and therefore contribute to the tellurium source term assessment.

2. Background

2.1. Aerosol properties

It was estimated in (Kissane, 2008) that aerosols in the primary circuit during a severe NPP accident would comprise a nearly lognormal population of particles. The aerodynamic mass median diameter (AMMD) of particles would be around 1 to 2 μm and geometric standard deviation around 2. The larger particles would consist for the most part of agglomerates, which would consist of compact clusters as small as 0.1 μm. It was also estimated in (Kissane, 2008) that the composition of particles would be of one-third metal, one-third metal oxide and one-third a mixture of mainly FP species. In the containment, particles are typically larger. These particles represent the particles formed in the primary circuit, as well as agglomerates of them. A smaller population of FP-rich particles may form e.g. at the breach in the event of a hot-leg sequence, thus creating a bimodal aerosol population in the containment. During such an event, FP species vapours would be released into the containment and either nucleate (creating a population of small particles rich in FPs) and/or condense onto existing aerosols. Secondary sources of aerosol material in the containment can contribute significantly in masses of aerosol to those of the primary source. For example, in the case of molten-core-concrete interaction (MCCI), the primary particles would agglomerate with the largely concrete-derived contribution. (Kissane, 2008)

2.2. Spray phenomena

The CSS has been found to be efficient in removing particulate FPs from the containment atmosphere (Hilliard & Postma, 1981; Dehjourian et al., 2016). The removal efficiency is dependent on several factors such as the composition of the spray solution and the particle size distribution of the FPs. The CSS is the most efficient at removing particles>1 μm or smaller than 0.1 μm (OECD/NEA, 2009), but the removal efficiency remains low for the accumulation mode particles (between 0.1 and 1 μm). For the larger particles, the most effective removal happens through impaction as they have sufficient inertia (Ardon-Dryer et al., 2015) and do not follow the streamline around the droplet but instead collide onto the surface of it. For the smaller particles, diffusion to the droplet surface is the most effective mechanism. (OECD/NEA, 2009; Sehgal, 2011) In this case, particles are more able to follow the streamlines of the flow field around a droplet. Brownian diffusion refers to the movement of the particle due to collisions with air molecules. Because these impulses are not perfectly balanced on the time scales of interest during the passage of a droplet, there is an apparent diffusion of aerosol particles leading to contact with the droplet (Powers and Burson, 1993). In between the size range of smaller and larger particles, the intermediate size particles (accumulation mode) are captured by the interception with the droplet, since the particles follow a streamline that approaches the droplet surface within a distance equivalent to the particle radius (Ardon-Dryer et al., 2015).

There are also other mechanisms affecting the particle removal, such as electrophoresis due to the charging of particles and droplets, e.g., in the radiation field and the subsequent attraction between the opposite charged objects. This phenomenon is important for the smaller particles. Other major phenomena are thermophoresis and diffusiophoresis, which take place when there is a temperature gradient between the droplet and surrounding atmosphere or when there is a concentration gradient in water vapor near an evaporating droplet, respectively. These phenomena are more important for the intermediate size range particles. The mathematical equations describing the removal efficiency due to the above-mentioned phenomena are summarized in (Ardon-Dryer et al., 2015).

There are also other factors that have an effect on the removal of particles (Ardon-Dryer et al., 2015), such as particle properties (e.g., density, shape), flow conditions (e.g., laminar, turbulent), the relative humidity of the containment atmosphere. Considering the spray droplet, the temperature of containment atmosphere and the droplet surrounding steam content are key factors defining the lifetime (drying time) of a droplet. A 10-μm water droplet lifetime has been estimated to be ca. 100 s at RH 100% and 0.1 s at RH 50% (and practically the same at RH 0%), when temperature is 293 K (Hinds, 1999). Similarly, for a 100-μm droplet, the lifetime is 10 s at RH 50% (and practically the same at RH 0%). In this work, the spray droplets mean size was approximately 10 μm in diameter (numerically), whereas the droplet mean size in a real nuclear power plant CSS is significantly bigger, falling within a range of several hundred micrometers while the droplet number size distribution ranges up to 2,000 to 3,000 μm (Powers and Burson, 1993). Therefore, the spray droplets in this work represented the lower range of spray droplets' size distribution, the efficiency of which for particle removal is not as well-known or studied as it is for the large droplets. In addition, it has been observed that the chemicals in spray solution, such as the addition of a boric acid-sodium hydroxide solution (3000 ppm boron; pH = 9.5), may result in much coarser droplet distributions than those obtained with water (Powers and Burson, 1993).

2.3. Containment spray chemistry

In addition to aerosol particles, gaseous species can be removed from the containment atmosphere by altering the chemistry of the spray solution to efficiently react with the gaseous compounds and convert them into non-volatile form (Ashmore et al., 1996). The CSS solution is generally composed of a base (e.g., sodium hydroxide, potassium hydroxide, trisodium phosphate), boric acid and possibly an additive (sodium thiosulphate, hydrazine) (Lavonen, 2014). The chemistry of the spray solution (e.g., alkaline pH, reducing additives) is optimized to mitigate and decompose iodine species. In alkaline pH, iodine will be in a form of non-volatile iodide and therefore will stay in the liquid phase (Ashmore et al., 1996). In addition, the additives used in the sprays are designed to trap volatile iodine inside the droplets and reduce it to a non-volatile form (Parsly, 1971). This way the droplets will not become saturated with volatile iodine and the release is mitigated. Lastly, boric acid is added to the spray to maintain subcriticality of the reactor core

during the recirculation phase (Neeb, 2011) as well as to buffer the alkaline pH. Aside from the boric acid, the additives added to mitigate the release of iodine may have different effects on other FPs. One such FP is tellurium, where the knowledge on the behavior of it in the containment is still relatively scarce (including the CSS). The chemical effect of the containment sprays with different compositions on tellurium has not been experimentally investigated. However, tellurium has a relatively complex chemistry and there is evidence that tellurium species in the sump are affected by the chemical additives used in the spray, especially under radiation (Pasi et al., 2020). Therefore, it is crucial to investigate the effect of chemistry applied by the sprays on tellurium retention and to assess potential drawbacks due to the additives added to the spray solutions. Furthermore, the current severe accident analysis codes do not fully cover these phenomena due to the lack of experimental data.

3. Methods and materials

3.1. Experimental setup

The schematics of the "VTT spray chamber" experimental setup is shown in Fig. 1. The setup consisted of a cylindrical spray chamber made of stainless steel, simulating a containment building. The inner walls of the chamber were coated with Teflon tape to passivate the surfaces. The dimensions of the chamber are given in the figure. A spray nozzle (model Lechler 136.330.xx.16) simulating a containment spray system was attached on top of the chamber. The spray droplets (ca. 10 μm in diameter) were generated from the solution in the spray supply bottle and the droplet feed rate was controlled with a pressurized air or nitrogen (usually 3 bar absolute). Therefore, the spray nozzle output was a mixture of droplets (feed rate 9.0 ml/min) and gas (25.4 l/min). Based on the data sheet of the manufacturer, the width of the spray cone was 60 mm at a distance of 150 mm from the spray nozzle, and 120 mm at a distance of 300 mm (at a spray angle of 20°). The temperature of spray solution and spray chamber was 293 K. The generated spray droplets accumulated at the bottom of the chamber, known as the sump.

Powdery tellurium precursor was vaporized in an alumina crucible place inside a stainless-steel tube (AISI 316l) of tubular furnace (Entech/Vecstar, VCTF 3). The experiments were conducted with two different tellurium precursors: tellurium dioxide (TeO$_2$, supplied by Sigma-Aldrich, purity $\geq$ 99%) and metallic tellurium (Te, supplied by Sigma-Aldrich, purity $\geq$ 99.997%). The mass of both precursors corresponds to 1 g of elemental tellurium, which for metallic tellurium was 1 g and tellurium dioxide was 1.26 g. The heating temperatures were chosen slightly above the melting points of the respective tellurium precursors, 810 K for Te and 1150 K for TeO$_2$. This provided a steady, long-term release of tellurium through the system into the containment model, which allowed a continuous experiment with multiple spray conditions. A flow rate of 5 l/min (air or nitrogen) through the furnace was adjusted to transport the vaporized tellurium compounds through a stainless-steel line (AISI 316l) to the entrance of the spray chamber. The steam content of the flow was adjusted by directing half of the flow upstream of the furnace via an atomizer generating droplets of water (MilliQ) in the supply bottle. The additional, airborne caesium iodide particles were produced in the same manner, mixing CsI powder with the water in the atomizer supply bottle (4 g of CsI in 100 g of water). Next, the generated droplets were directed into the furnace, in which the droplets dried, and solid CsI particles were formed. The flow cooled down to ca. 293 K before entering the vertical spray chamber through a connection in the lower section.

Inside the spray chamber, the aerosols were subjected to the spray droplets. In terms of the sprays, three different solutions were used: **I.** 18 MΩ deionized MilliQ water (Millipore), **II.** Alkaline borate solution (0.23 M H$_3$BO$_3$, 0.15 M NaOH) **III.** Alkaline borate solution with sodium thiosulphate (0.23 M H$_3$BO$_3$, 0.15 M NaOH and 0.064 M Na$_2$S$_2$O$_3$). The pH of both of the chemical spray solutions was around 9.3, whereas pH was close to neutral for MilliQ water. The chemicals were chosen to represent the general composition of the spray solutions used in severe accident scenarios (Bishop and Nitti, 1971; Hilliard et al., 1971). The aerosol flow not captured by the spray droplets exited close to the top of the spray chamber. Downstream of this exit, the aerosol flow was diluted and dried with a hot gas flow (21.5 l/min) of air or nitrogen (373 K), thus avoiding water condensation in the line and decreasing aerosol losses on the line surfaces. Aerosols were filtered out after the hot dilution (at a location with a temperature of 303 K). The plane filter was 47 mm in diameter (MilliPore, Mitex™ PTFE, pore size 5 μm). Beyond the filter, a 0.1 M sodium hydroxide trap (volume 300 ml) was positioned to ensure retention of any gaseous
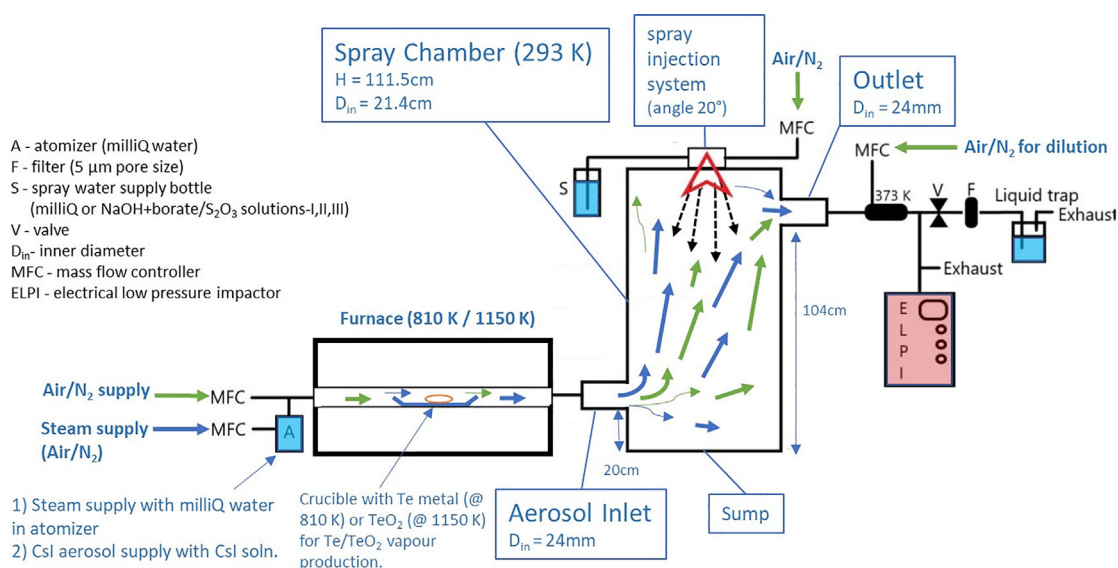

Fig. 1. Schematics of the experimental setup for the studies on the tellurium retention by containment spray system.

tellurium species possibly released through the setup. The flow rate through the filter and trap was 1.0 l/min. The aerosol properties in the gas phase were also monitored online using an Electrical Low Pressure Impactor (ELPI), further details are given below. The remaining gas flows were directed to the exhaust line.

All gas flows were controlled using mass flow controllers (Brooks S5851, Brooks® Instrument). However, the spray nozzle gas flow, generating the suction of the spray liquid from the supply bottle and further atomization in the spray nozzle, was controlled with an MFC coupled with a pressure meter (Drück, DPI 101 Digital Pressure Indicator).

3.2. Analytical methods

3.2.1. Tellurium release

A constant gas flow was directed over the crucible inside the furnace, thus enabling stable release conditions for the tellurium precursor. The mass loss/release of the precursor in the crucible was determined by weighing the crucible in the beginning and at the end of each experiment.

3.2.2. Electrical Low Pressure impactor (ELPI)

The mass size distribution of particles was measured online with an Electrical Low Pressure Impactor (Classic ELPI®, Dekati Ltd model 97 2E) with a time resolution of 1 s. Inside the ELPI, particles were charged with a corona charger and then differentiated by their aerodynamic diameter on twelve impaction stages inside the cascade impactor. The aerodynamic diameter is defined as the diameter of a spherical particle with a density of 1 g/cm³ (the density of a water droplet) that has the same settling velocity as the measured particle (Hinds, 1999). The number concentration of particles on each impaction stage was derived from the electrical charge of particles and the measured electrical current from the stages, which was mathematically converted to the form of mass concentration data. The inlet of the impactor was at ca. atmospheric pressure and the outlet was at 100 mbar (absolute). The flow rate through ELPI was 9.75 l/min. The measurement range of the ELPI was from ca. 7 nm to 10 μm (less than 5 size channels per decade). The electrical filter stage of ELPI was used to enhance the nanoparticle measurement. Moreover, the midpoint of the particle size range instead of the cutoff diameter of each impactor stage was used for graphical presentation in this work. The measurement uncertainty was ± 10%. The measurement system was controlled with the ELPIVI software, version 4.0 (Dekati Ltd).

3.2.3. Scanning and Transmission electron microscopy

Particulate aerosol samples were collected on 400 mesh, perforated carbon film-coated copper grids (Agar Scientific), which can be analysed using Scanning Electron Microscopy (SEM). The particulate sampling was performed directly from the gas phase by passing a sample flow of 0.5 l/min through the grid. The particle sampler was connected to the exhaust line during the sampling. The size and morphology of the collected particles were analysed using scanning electron microscopy (SEM, Zeiss Crossbeam 540). SEM operated at 2.0 kV and the probe current was ca. 100 pA during imaging. In addition to the SEM imaging, the samples with caesium iodide additive were analysed for elemental composition by TEM (Transmission Electron Microscope, TALOS™ F200X (S)TEM). The TEM was operated in a scanning mode (STEM) at 200 kV with a probe current of ca. 100 pA. The analysis of elemental composition of the particle samples by EDX was performed using 30 cm² silicon drift detectors (SSD, Thermo Fisher Scientific/Bruker Super X 4-detector assembly).

3.2.4. Instrumental neutron Activation analysis (INAA)

The tellurium content on the filters was measured with Instrumental Neutron Activation Analysis (INAA). The filters were irradiated in the experimental reactor LVR-15 at Řež (Research Centre Řež, Ltd., Czech Republic) with a thermal neutron flux of $2.9 \cdot 10^{13}$ cm$^{-2} \cdot$s^{-1}, epithermal neutron flux of $1.0 \cdot 10^{13}$ cm$^{-2} \cdot$s^{-1}, and fast neutron fluence ($1.0 \cdot 10^{13}$ cm$^{-2} \cdot$s^{-1}). The activity in the irradiated samples was measured with a high-purity germanium (HPGe) detector (Genie 2000, Canberra). The sample preparation and detailed methodology is presented elsewhere (Kučera et al., 2020).

3.2.5. Inductively coupled Plasma mass Spectrometer (ICP-MS)

The tellurium concentration in the liquid trap samples was measured with an Inductively Coupled Plasma Mass Spectrometer (Thermo Scientific™ iCap Q ICP-MS). The samples were diluted to 1:10 with 0.5 M HNO₃ (Suprapure®, Merck). Rhodium (Ultra Scientific) was used as an internal standard. Tellurium standards were diluted from 10 ppm Te in HCl solution (High-Purity Standards). The software used to evaluate the data was the Qtegra™ Intelligent Scientific data solution (v.2.21465.44).

3.3. MELCOR modelling

MELCOR is a computer code that models the progression of severe accidents in nuclear power plants. MELCOR code version 2.2 was used in this work. The containment spray model in MELCOR calculates the heat and mass transfer between spray water droplets and the atmosphere. The model assumes that the droplets are spherical and isothermal and fall through the vessel at their terminal velocity without any horizontal velocity component. The model calculates aerosol removal by diffusiophoresis, inertial interception and impaction, and Brownian diffusion. The aerosol washout model may give non-physical results if a droplet size distribution is used. Therefore, the Users' Guide recommends using only a single-spray droplet size in aerosol washout calculations. (Humphries et al., 2019)

In principle, the spray used in the experiments should form a cone with the angle of 20°. However, the droplet size was so small that the droplet trajectories were distorted by the air flow after travelling a distance of 10 to 20 cm, and a cone was not formed. Instead, the droplets filled the whole test vessel, rather like fog. Therefore, the whole test vessel was modeled as a single control volume. The outlet from the vessel was modeled as a flow path, leading to a time-independent control volume at the atmospheric pressure. The vessel floor and wall were modelled as heat structures, even though only a tiny amount of aerosols deposited onto the structures.

The aerosol particles and the air were injected into the vessel as mass sources. The AMMD of the particles and the standard deviation were extracted from the ELPI measurement data. The spray droplet size was set to 18 μm, which is the Sauter mean diameter, according to the spray nozzle specifications.

The model was run for 1000 s without the spray and then another 1000 s with the spray, to ensure that the calculation had reached a steady state. The results were taken from the last 100 s.

3.4. Experiments and procedure

Overall, nine experiments were performed under different conditions. Experiments 1 to 7 were performed as individual experiments. However, Experiments 8 and 9 were performed with a continuous tellurium feed using the same precursor to observe the effect of CsI feed on the tellurium behaviour with the aim of keeping the experimental conditions otherwise as similar as possible between these two experiments. The experimental matrix is presented in Table 1. The parameters altered in the experiments

Table 1
Experimental matrix with the varied parameters.

Experiment[#]	Precursor	Temperature[K]	Atmosphere	Humidity[a]	CsI[b]
1	TeO_2	1150	Air	No	No
2	TeO_2	1150	Air	Yes	No
3	TeO_2	1150	Air	Yes	Yes
4	Te	810	Air	No	No
5	Te	810	Air	Yes	No
6	Te	810	Air	Yes	Yes
7	Te	810	Nitrogen	No	No
8	Te	810	Nitrogen	Yes	No
9	Te	810	Nitrogen	Yes	Yes

[a] Humidity content of the gas flow that entered the spray chamber was 21,000 ppmV
[b] CsI content of the atomizer supply bottle was 0.15 M

were precursor, furnace temperature, atmosphere, humidity and the feed of additional caesium iodide particles. In addition, three different spray solutions were used in each experiment: **I.** 18 MΩ deionized MilliQ water (Millipore), **II.** Alkaline borate solution (0.23 M H_3BO_3, 0.15 M NaOH) **III.** Alkaline borate solution with sodium thiosulphate (0.23 M H_3BO_3, 0.15 M NaOH and 0.064 M $Na_2S_2O_3$). The pH of both chemical spray solutions was around 9.3, whereas pH was close to neutral for MilliQ water.

Each experiment started by setting the desired gas flows and heating up the setup (furnace with precursor, hot dilution). After the stabilization of temperature and precursor feed rate, the first experimental condition was to collect a reference sample where all of the tellurium species transported through the system without the spray were collected on the filter and in the trap. In the next step, the three different spray solutions were tested separately. Each spray duration was 20 min. Filter and liquid trap samples were collected for further analyses under all studied conditions. Scanning electron microscopy samples were only collected in the reference condition. In addition, the spray pressure defining the spray droplet feed rate was also briefly varied to verify its impact on the tellurium removal efficiency (not shown in Table 1). However, this was only monitored online using ELPI (which was also monitoring the aerosol's behaviour in all studied conditions). The increase of spray pressure from 3 to 3.5 bar (absolute) increased the spray solution feed rate to 13.2 ml/min and the gas flow through the spray nozzle to 29.7 l/min.

4. Results

4.1. Feed rates of precursors

The feed rates of tellurium and additional CsI precursors are given in Table 2. The results are based on the INAA analysis of tellurium transported to filter in reference condition and on the feed rate of CsI solution using an atomizer monitored with the ELPI. Further discussion on the uncertainties in the precursor mass balance is given in Chapter 4.4.

Table 2
Feed rates of tellurium (given as metallic Te) and additional CsI precursors.

Experiment[#]	Tellurium precursor	Te[mg/min]	CsI[mg/min]
1	TeO_2	0.6	–
2	TeO_2	1.5	–
3	TeO_2	1.5	0.2
4	Te	1.0	–
5	Te	0.1	–
6	Te	0.7	0.2
7	Te	1.3	–
8	Te	0.9	–
9	Te	0.5	0.2

4.2. Properties of Te aerosols leaving the spray chamber

4.2.1. Particle online analysis using ELPI

The properties of tellurium aerosols in the different phases of experiments were monitored online using the ELPI: reference condition (without spray) and three spray conditions (with spray). The average mass size distributions describing the aerosol properties leaving the spray chamber without spray operation, corresponding to the reference condition, are shown in Fig. 2. Similarly, the average mass size distribution of the fed caesium iodide aerosol (without the feed of tellurium aerosols) is also shown in the figure. In general, the AMMD of tellurium aerosols was less than 1 μm. However, the particles formed large agglomerates, which extended the mass size distribution towards the particle diameters of several μm. In proportion to the total tellurium aerosol mass concentration, the fraction of agglomerates seemed to be more pronounced in the experiments with metallic tellurium precursor (see SEM analysis results in Chapter 4.2.2). The mass concentration of tellurium aerosol particles varied between the experiments and the highest concentration was observed in the experiments with a tellurium dioxide precursor. In Experiment 5 (metallic tellurium precursor in humid air), the mass concentration was very low and a possible error in the experiment is suspected. The airborne caesium iodide aerosol additive was fed together with tellurium aerosols in Experiments 3, 6 and 9. The AMMD of CsI aerosol was approx. 1.5 μm. It seemed that the mass size distributions of tellurium aerosols grew wider due to the CsI particles.
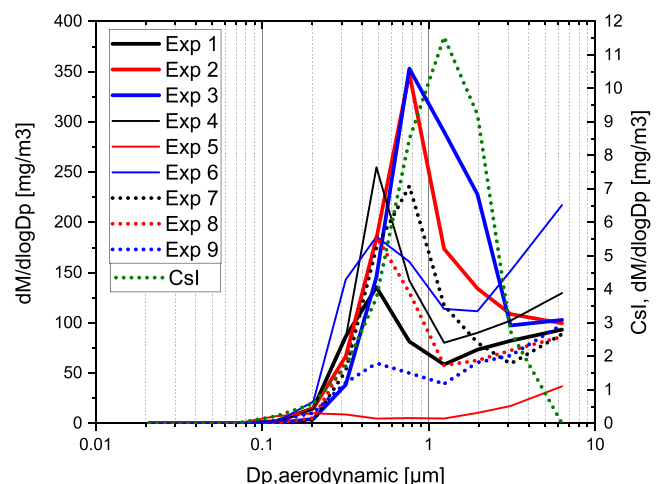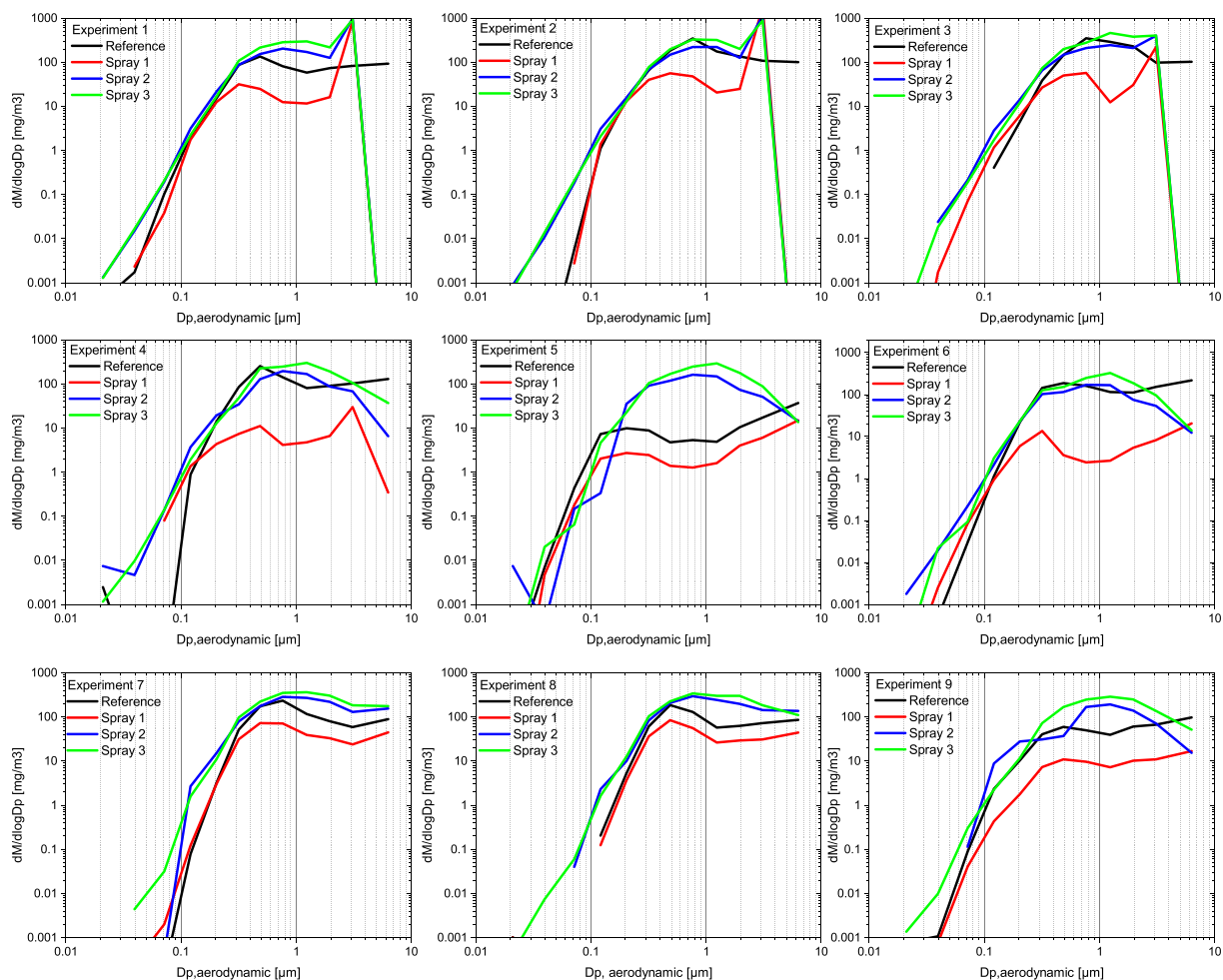

Fig. 2. Average mass size distributions of the fed tellurium aerosols leaving the spray chamber (without spray) - reference condition. Caesium iodide aerosol was fed together with tellurium aerosols in Experiments 3, 6 and 9. The average mass size distribution of the fed caesium iodide aerosol is also shown.

A collection of the average mass size distributions of the fed tellurium aerosols during reference condition (without spray) and while testing three different spray solutions (with spray) leaving the spray chamber is shown separately for each experiment in Fig. 3. The effect of spray droplets generated from MilliQ water for decreasing the transport of particles through the spray chamber was evident in all experiments. The transport of tellurium aerosols was notably hindered for particles with an aerodynamic diameter larger than ca. 0.2 μm. For smaller particles, the transport did not seem to change significantly. In the case of chemical (alkaline) spray droplets, the effect on the particle transport through the spray chamber was not clear anymore. The droplets likely captured tellurium aerosols efficiently, but it could not be deduced from the obtained mass size distribution data. It seemed that the feed of chemical droplets increased the particle transport and a new, wide peak in the mass size distribution was observed for particles with a mode (aerodynamic) diameter in the range of 0.8 to 1.3 μm. The mode diameter and mass concentration increased with the increased amount of chemicals in the droplets (from H_3BO_3 and NaOH to H_3BO_3, NaOH and $Na_2S_2O_3$). In addition, the particle transport through the spray chamber was also notably increased in the case of chemical droplets for particles with an aerodynamic diameter less than ca. 0.2 μm (could also be primarily related to the shift of aerosol distribution towards smaller sizes due to the decreased coagulation/agglomeration of particles after the washout of airborne particles by the spray droplets). Therefore, it seemed that

the chemical droplets were actually forming the observed aerosol particles while the droplets were drying in the experimental setup. Likely, a peak formed by the droplets was observed with an aerodynamic diameter of ca. 3.1 μm. The peak was clearly visible in the experiments with tellurium dioxide precursor, but it was less pronounced in the experiments with metallic tellurium precursor. It could be that the peak was formed by the drying droplets and TeO_2 particles/agglomerates captured within the droplets. This would be further supported by the fact that the spray droplets were originally 10 μm in diameter and therefore, notably larger than the observed peak diameter in the distribution.

The likelihood of an experimental error in the feed of tellurium precursor in Experiment 5 was further supported by the low mass concentration during the reference condition in comparison to the feed of chemical droplets, which remained on the same level as in other experiments (see Fig. 3). In general, the tellurium mass size distribution at least partially overlapped with the distribution of chemical droplets, but the difference between the distributions was significant in Experiment 5. However, the X-ray diffraction analysis of the remaining tellurium precursors in the crucible after the experiments (shown in the Supplementary file S1) verified that the precursor in Experiment 5 contained a significant fraction of metallic tellurium. It verified the use of a correct precursor and therefore, Experiment 5 has been included in the presentation of results from this work.

Fig. 3. Average mass size distributions (log–log scale) of the fed tellurium aerosols during reference condition (without spray) and while testing three different spray solutions (with spray) leaving the spray chamber. Spray 1: MilliQ water, Spray 2: MilliQ water, H_3BO_3 and NaOH solution, Spray 3: MilliQ water, H_3BO_3, NaOH and $Na_2S_2O_3$ solution. Caesium iodide aerosol was fed together with tellurium aerosols in Experiments 3, 6 and 9.

4.2.2. Particle analysis using SEM

The particle samples were collected on grid substrates during the reference condition (no spray) in each experiment. The SEM micrographs of the collected particles are shown in Fig. 4 for each experiment. In Fig. 4, a, b and c correspond to the experiments with TeO$_2$ aerosol in air (Experiments 1, 2 and 3, respectively), d, e and f to the experiments with metallic Te aerosol in air (Experiments 4, 5 and 6, respectively) and g, h, i to the experiments with metallic Te aerosol in nitrogen (Experiments 7, 8 and 9, respectively). In all experiments, the abundant formation of long agglomerate chains (>100 nm) in the gas phase had taken place before the particle collection on grids. The agglomerates were composed of primary particles (less than100 nm), the primary particles seemed to be smaller in the experiments with metallic Te. The images are mostly from the less loaded areas of the specimen. The fraction of large, spherical, individual particles (>100 nm) was the highest in Experiments 1 to 3. In addition, the primary particles were somewhat fused together in Experiments 1 to 3. In Experiments 4 to 6, performed with metallic Te in an air atmosphere, the agglomerates were typically long chains of spherical particles with varying primary particle sizes (particle size less than 50 nm). However, under humid conditions when caesium iodide aerosol additive was introduced into the gas flow, the morphology of spherical particles was lost. In Experiments 7 to 9, performed with metallic Te in a nitrogen atmosphere, the formation of agglomerates was obvious. In humid condition with caesium iodide aerosol additive, growth of thick, needle-like crystals was observed. These crystals seemed to collide and coagulate with the tellurium aerosol. Based on the EDX analysis using TEM, only tellurium and oxygen was detected in the crystals. In a second SEM sample collected at the end of Experiment 9 (not shown in the figure), the number concentration of tellurium agglomerates had decreased, indicating a decreased release of precursor. In addition, the morphology of particles was

lost due to humid conditions prevailing in the setup after the spray conditions. In general, only tellurium and oxygen were observed in the particle samples of Experiments 3, 6 and 9 (with the feed of airborne CsI particles) indicating the speciation of tellurium oxides (Te$_x$O$_y$). The oxygen content of the particles seemed to be higher for the experiments in the air atmosphere than in the nitrogen atmosphere with steam. Due to the overlap of relevant (L lines) Cs and I peaks with the Te peaks in the EDX analysis, it is difficult to make a conclusion on the content of Cs and I in the formed particles.

4.3. Tellurium captured on filter and removal efficiency

The mass of tellurium aerosols captured on the filter downstream of the CSS are listed in Table 3 (based on the INAA analysis data (Kučera et al. 2020)). The tellurium transport in a gaseous form to the liquid trap could not be accurately analysed due to the low mass, which was at or below the detection limit of INAA and ICP-MS. Therefore, a total sample containing all four experimental conditions was collected to estimate the gaseous transport of tellurium (see Table 3). This sample indicated low concentration of any gaseous tellurium species, partly due to the rather high dilution of the formed gaseous species within the spray chamber and further downstream of the chamber diluting the sample flow (extracted from the main flow) directed to the liquid trap. Since the aerosol filter and gaseous trap samples were representing only the gas flow with airborne particles through the sampling line to the filter and trap, the sampling results were converted to the corresponding total particle and gas transport out of the spray chamber considering the total gas flow rate downstream of the chamber.

Similarly, the masses of Cs and I bound to particles captured on the filter downstream of the CSS are listed in Table 4 (based on the INAA analysis data (Kučera et al. 2020)). The caesium and iodine
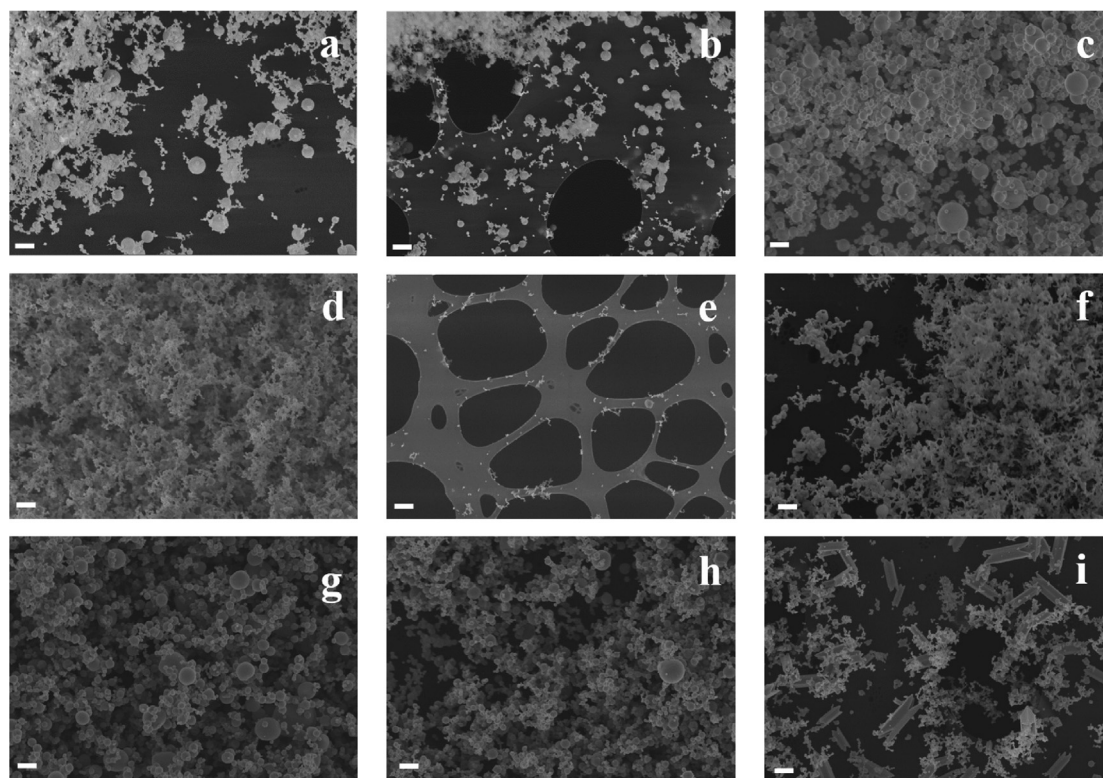
Fig. 4. SEM micrographs of the experiments conducted in air: a) Experiment 1, b) Experiment 2, c) Experiment 3, d) Experiment 4, e) Experiment 5 and f) Experiment 6 and in nitrogen g) Experiment 7, h) Experiment 8 and i) Experiment 9. The scale bar is 300 nm in each experiment. In Experiments 1 to 3, the precursor was TeO$_2$. In Experiments 4 to 9, the precursor was metallic Te. Additional CsI particles were fed in Experiments 3, 6 and 9.

Table 3

Tellurium aerosol captured on the filter and in the trap - given as metallic tellurium. The total tellurium transport results downstream of the spray chamber were calculated based on the filter and trap sample results. The removal efficiency results derived from the filter samples comparing the reference and spray conditions are shown. Note: the trap samples contained <u>all gaseous tellurium collected during all four conditions</u>. The presented results are based on the INAA analysis. Reference: no spray, Spray 1: MilliQ water, Spray 2: MilliQ water, H_3BO_3 and NaOH solution, Spray 3: MilliQ water, H_3BO_3, NaOH and $Na_2S_2O_3$ solution.

Experiment [#]	Conditions	Te on filter [μg]	Te transport as aerosol in total [μg]	Te transport as aerosol in total [μg/min]	Removal efficiency [%]	Te in trap [μg]	Te transport as gas in total [μg]
1	Reference	240	12,350	618	–	0.4	22.3
	Spray 1	42	2160	108	82.5	–	–
	Spray 2	10	510	26	95.8	–	–
	Spray 3	8	410	21	96.7	–	–
2	Reference	570	29,330	1467	–	0.3	17.8
	Spray 1	69	3550	178	87.9	–	–
	Spray 2	16	820	41	97.2	–	–
	Spray 3	16	820	41	97.2	–	–
3	Reference	588	30,250	1513	–	0.3	13.1
	Spray 1	47	2420	121	92.0	–	–
	Spray 2	13	670	34	97.8	–	–
	Spray 3	13	670	34	97.8	–	–
4	Reference	373	19,190	960	–	0.4	19.9
	Spray 1	63	3240	162	83.1	–	–
	Spray 2	2	100	5	99.5	–	–
	Spray 3	2	100	5	99.5	–	–
5	Reference	23	1180	59	–	0.4	19.2
	Spray 1	6	310	16	73.9	–	–
	Spray 2	7	360	18	69.6	–	–
	Spray 3	3	150	8	87.0	–	–
6	Reference	283	14,560	728	–	0.4	19.0
	Spray 1	20	1030	52	92.9	–	–
	Spray 2	2	100	5	99.3	–	–
	Spray 3	2	100	5	99.3	–	–
7	Reference	497	25,570	1279	–	0.2	12.2
	Spray 1	180	9260	463	63.8	–	–
	Spray 2	138	7100	355	72.2	–	–
	Spray 3	125	6430	322	74.8	–	–
8	Reference	348	17,900	895	–	0.2[a]	9.3
	Spray 1	150	7720	386	56.9	–	–
	Spray 2	128	6590	330	63.2	–	–
	Spray 3	107	5510	276	69.3	–	–
9	Reference	177	9110	456	–	0.2[a]	9.3
	Spray 1	17	870	44	90.4	–	–
	Spray 2	9	460	23	94.9	–	–
	Spray 3	7	360	18	96.0	–	–

[a]Experiments 8 and 9 were performed with a continuous tellurium feed using the same precursor, thus the subsequent accumulated mass of tellurium in the liquid trap sample was divided in half-and-half to estimate the mass of tellurium in liquid trap samples of each experiment.

Table 4

Caesium and iodine bound to particles captured on the filter. The total caesium and iodine transport results downstream of the spray chamber were calculated based on the filter sample results. The removal efficiency results derived from the filter samples comparing the reference and spray conditions are shown. The presented results are based on the INAA analysis. Reference: no spray, Spray 1: MilliQ water, Spray 2: MilliQ water, H_3BO_3 and NaOH solution, Spray 3: MilliQ water, H_3BO_3, NaOH and $Na_2S_2O_3$ solution.

Experiment [#]	Conditions	Cs on filter [μg]	Cs transport as aerosol in total [μg/min]	Removal efficiency [%]	I on filter [μg]	I transport as aerosol in total [μg/min]	Removal efficiency [%]
3	Reference	8	21	–	0.5	2	–
	Spray 1	3	8	64.1	0.4	1	32.7
	Spray 2	2	6	73.1	4	9	–
	Spray 3	2	4	78.8	0.3	1	50.4
6	Reference	17	45	–	16	43	–
	Spray 1	2	7	85.5	2	6	85.0
	Spray 2	3	8	82.6	3	7	83.2
	Spray 3	9	23	47.3	9	25	42.4
9	Reference	11	30	–	12	31	–
	Spray 1	3	7	75.8	3	8	73.4
	Spray 2	7	18	40.0	8	20	35.5
	Spray 3	2	4	86.6	2	5	85.4

transport in a gaseous form to the liquid trap could not be accurately analysed due to the low mass, which was at or below the detection limit of INAA and ICP-MS. Since most of the fed CsI is expected to be transported as particles at low temperatures (corresponding to the spray chamber outlet), the subsequent masses of Cs and I gaseous fractions would be even lower than the masses of the analysed particle fractions (Table 4).

The results for tellurium, caesium and iodine removal efficiencies by the containment spray system, shown in Tables 3 and 4, were derived based on the aerosol transport results during the reference condition and the subsequent spray conditions. The removal efficiencies for tellurium particle fraction are also shown in Fig. 5. The results for tellurium and caesium trapped in the sump in Experiments, 3, 6 and 9 are shown in the Supplementary file S1.
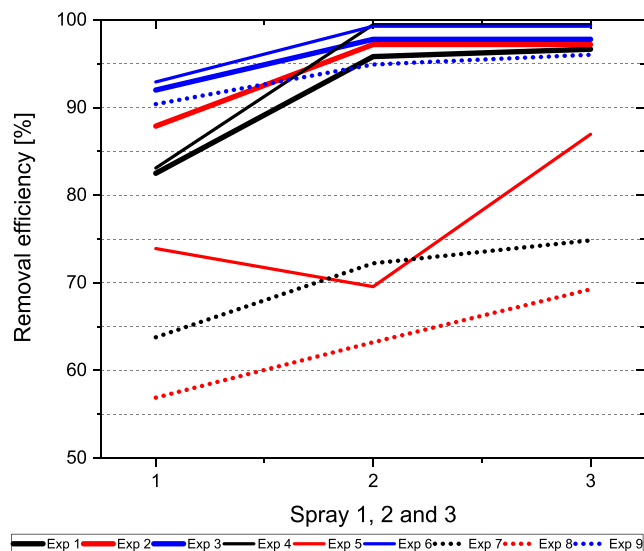
Fig. 5. Removal efficiency for the tellurium aerosols in Experiments 1 to 9. A possible experimental error in Experiment 5 is suggested. Spray 1: MilliQ water, Spray 2: MilliQ water, H_3BO_3 and NaOH solution, Spray 3: MilliQ water, H_3BO_3, NaOH and $Na_2S_2O_3$ solution.

A clear trend in the improvement of tellurium removal efficiency when switching on the spray and then adding chemicals to the spray solution was observed, as seen in Fig. 5. In most of the cases, the removal efficiency was above 80% using MilliQ water spray droplets. The chemical spray droplets increased the efficiency above 95%. Further addition of chemicals improved the efficiency somewhat. The removal of the tellurium aerosols TeO_2 and metallic Te was rather similar in the air atmosphere when spraying water droplets - the possibility of metallic Te oxidation to TeO_2 was suggested. Metallic Te removal seemed to be improved more than TeO_2 when feeding the chemical spray droplets. However, the removal efficiency of metallic Te decreased drastically in the nitrogen atmosphere. This observed behaviour should be further investigated. In all atmospheres, the additional airborne CsI particles (Experiments 3, 6 and 9) increased the removal efficiency. The phenomenon was particularly notable in the air atmosphere when using water droplets. In the cases of chemical droplets, the effect was not as high. Interestingly, the metallic tellurium removal efficiency in the nitrogen atmosphere increased from 55–75% to 90–95% due to the CsI particles. It indicated that the additional CsI particles (and the chemical droplets or the dried residue of them) were likely colliding/coagulating with the tellurium aerosols and thus improving their removal in all experiments. However, the effect of CsI particles in Experiment 9 was notably higher and the removal efficiency due to CsI was on practically the same level in all spray conditions. The possibility of a chemical reaction between Te and CsI should be considered; it likely took place inside the furnace, in which the reaction temperature was high. An SEM micrograph of Experiment 9 (in Fig. 4) indicated the formation of long, large crystals due to the addition of CsI. Further EDX analysis indicated that the crystals were composed of tellurium and oxygen - no Cs or I could be detected, but their role in formation of the crystal cannot be ruled out. The crystals coagulated with the tellurium aerosol. These crystals/particles may have significantly enhanced the removal efficiency for tellurium. In addition, the feed of steam (in carrier gas) seemed to decrease the removal efficiency for metallic Te particles, although the data of Experiment 5 is somewhat uncertain to draw a solid conclusion. Metallic tellurium is insoluble in water, which further supports the observation. In addition, based on the XRD analysis of tellurium precursor after the

experiments (see the Supplementary file S1), the precursor from Experiment 5 exhibited more distinctive signals of metallic Te, indicating a higher fraction of metallic tellurium compared to the precursors from Experiments 4 and 6 with a significant fraction of tellurium oxidized to TeO_2. This could indicate a different behaviour of metallic tellurium in humid air compared to dry air or humid air with additional CsI particles. Considering the transport of gaseous tellurium species through the spray chamber to the trap, the accumulated mass of tellurium in the trap solution of each experiment (covering four different conditions) was very low, see Table 3. It indicated that gaseous tellurium species were likely existing in the experiments, but their mass concentrations were negligible in comparison to the mass concentrations of the particulate tellurium species.

The removal efficiencies for Cs and I were in a good agreement in Experiments 6 and 9 (using metallic tellurium precursor), see Table 4. The removal efficiency ranged up to approx. 86% for both elements. However, at some of the experimental conditions the obtained removal efficiency was low (36–47%), which is interpreted to be rather due to the uncertainties in the experiments and analyses than due to the experimental conditions.

In Experiment 3, where TeO_2 was used as the precursor in the air atmosphere, the removal efficiencies for Cs and I were generally lower than in the experiments using metallic tellurium precursor. The removal efficiency for Cs ranged from 64% to 79%, whereas the removal efficiency for I was lower being in a range from 33% to 50%. One suggestion is that in the oxidizing atmosphere, iodide was oxidized to gaseous species I_2 which cannot be removed as efficiently as particulate species. In this case, the molecular iodine could have passed the filter into the liquid trap. However, the concentration of iodine in the liquid trap was too low to be detected and therefore, the effect of iodine oxidation to the removal efficiencies cannot be fully concluded. The removal efficiencies for Cs and I seemed to increase with the addition of chemicals and the highest removal efficiency was observed when thiosulphate was present.

Based on the INAA analysis results, it seemed that gaseous iodine was mainly formed in Experiment 3, in which the furnace temperature was also higher due to the use of TeO_2 precursor, thus enabling an efficient vaporization of CsI. Otherwise, based on the rather even masses of Cs and I in the filter samples of Experiments 6 and 9, both elements were transported to the filter in the form of CsI particles.

Overall, it is difficult to differentiate the improvement in the removal efficiency of the investigated tellurium aerosols due to the chemical effect of spray droplets. The reason for the improvement could be the increased collision/interception with the spray aerosols (droplets, dry residue) and coagulation/adsorption, thus a physical phenomenon. In addition, the mean size of the fed CsI particles was larger than of tellurium aerosols, especially in the case of metallic tellurium precursor. It may have improved the coagulation of tellurium aerosols with caesium iodide particles, thus enhancing the removal efficiency due to the spray droplets (see Fig. 2). Especially the large crystals observed in Experiment 9 likely improved the tellurium aerosol removal efficiency. However, it is known that metallic tellurium is insoluble in water, whereas tellurium dioxide is barely soluble in water. Therefore, the spray droplets may have increased the retention of tellurium in the form of TeO_2 particles (originated from the TeO_2 precursor or via oxidation of the metallic Te precursor into TeO_2) via dissolution in the experiments. In addition, the nano- and micro-sized particles may have a higher solubility / hygroscopicity than the bulk material (Dora et al., 2010), but that was not investigated in this work. In general, when comparing the reference conditions of all experiments, it seems humidity increased the release and thus transport of tellurium aerosol in the air atmosphere for TeO_2 precursor. In the case of metallic Te in the air and nitrogen

atmosphere, the release and thus transport of tellurium aerosol was decreased in humid conditions, see the Supplementary file S1.

The chemical effect may be significant for the removal efficiency of gaseous species, but in these experiments, the gaseous fraction of tellurium species was very low and it was not possible to make any conclusions. On the other hand, the collision of tellurium aerosols with the spray aerosols may also lead to a further chemical reaction between the tellurium and chemicals in the spray droplets. Furthermore, the chemicals will also enhance the propensity of tellurium retention when the mixture of tellurium and spray droplets have settled down from the containment atmosphere and deposited onto the surfaces/water pools of the containment building.

The CSS removal efficiency for tellurium aerosols was also estimated based on the online data of ELPI measurements. The particle number concentration data was converted to mass concentration data and the derived removal efficiency as a function of a particle's aerodynamic diameter is shown for the case of MilliQ water spray droplets in Fig. 6. In case of the water spray droplets, the removal efficiency was on the same level as was obtained based on the INAA analysis, thus verifying the results. The removal efficiency formed a plateau at the location of the tellurium aerosol feed mass size distribution. However, in the upper size range of the distribution, the water spray droplets seemed to be interfering with the measurement data. Likely, the spray droplets coagulated with TeO_2 particles/agglomerates and caused further increased aerosol transport downstream of the CSS. Therefore, the removal efficiencies for the particles bigger than 2 μm in aerodynamic diameter decreased in the case of TeO_2 aerosol. Another option would be that the water droplets alone interfered the ELPI measurement in Experiments 1 to 3. In general, similar behavior was not observed for metallic Te aerosol and thus, the removal efficiency remained on a rather constant level. However, a slight dip was observed in Experiment 4 performed with metallic tellurium in the air atmosphere - the role of tellurium oxidation into tellurium dioxide on the similarity of the obtained removal efficiency decrease was suspected. In the lower size range of the distribution, particles less than 0.5 μm in aerodynamic diameter, the removal efficiency decreased significantly. This could be related to the fact that particles with a diameter in the range of 0.1 to 0.3 μm are generally difficult to trap. On the other hand, the feed mass concentration of tellurium aerosols was also low and decreased in that size range, which interferes the reliable analysis of removal efficiency.

In the case of chemical spray droplets, the removal efficiency of CSS for tellurium aerosols could not be derived based on the ELPI online data. The fed chemicals were forming measurable particles, which also overlapped with the size range of tellurium aerosols and thus, they were recorded in the ELPI measurement data decreasing the obtained removal efficiency results.

As an additional feature in the experiments, the effect of higher spray pressure was tested for the MilliQ water spray condition. In general, the spray operation pressure was 3 bar(a), but the pressure was increased to 3.5 bar(a) for a while and the impact on the measured tellurium aerosol data was online monitored using ELPI. The higher pressure increased the spray solution feed rate and also increased the total gas flow through the setup. The effect on the removal efficiency was examined and a spray removal improvement factor as a function of particle aerodynamic diameter was derived, as shown in Fig. 7. In all experiments, at the area of fed aerosol mass size distribution, the higher spray pressure improved the removal efficiency of tellurium aerosols. The highest improvement was observed for the experiments in the air atmosphere; especially for the TeO_2 aerosol, an improvement by a factor of up to 4.5 was recorded. For the metallic Te aerosol, the improvement of removal efficiency reached up to a factor of 2.5. In the nitrogen atmosphere, the removal efficiency was only slightly higher than in the case of lower spray pressure. The effect of atmosphere on the results is interesting and further studies would be needed to verify whether the nitrogen atmosphere induces phenomena effecting tellurium behavior. On the other hand, the oxidation of tellurium is mainly avoided and thus, the results already differ from the case of air atmosphere. In the air atmosphere, most of the particles formed from the metallic precursor were likely oxidized to TeO_2.

4.4. Mass balance and uncertainties in the experiments

The mass balance and uncertainties in the experiments are discussed in the Supplementary file S1. To summarize, the mass balance was not easy to extract for all experiments. The obtained results showed that there is no issue that would cause tellurium
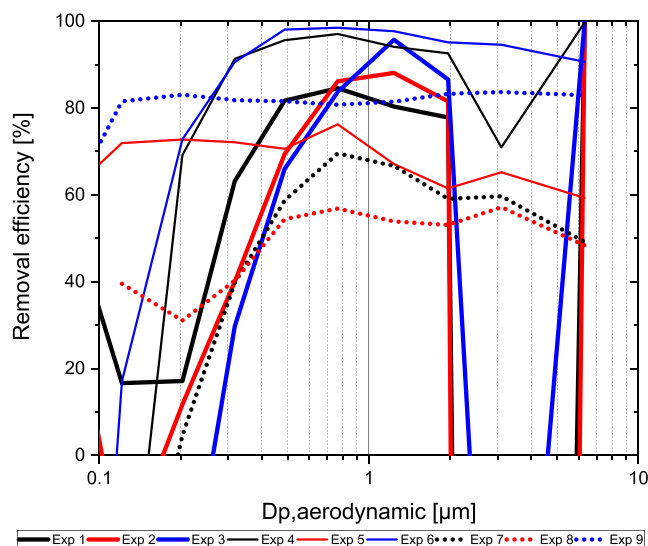
Fig. 6. Removal efficiency of the tellurium aerosols in Experiments 1 to 9. The results are based on the ELPI online measurement data and shown as a function of particle aerodynamic diameter. The results cover only the condition of MilliQ water spray droplets.
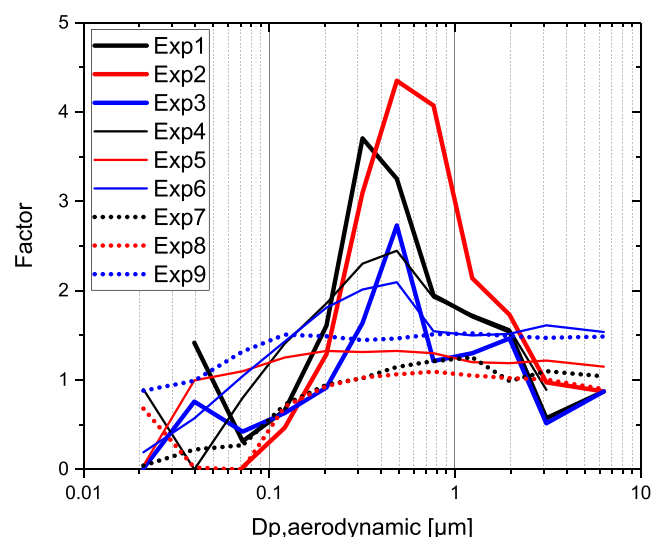
Fig. 7. Spray removal improvement factor as a function of particle aerodynamic diameter, when the spray pressure was increased from 3 to 3.5 bar(a) (the conditions of MilliQ water spray droplets). The effect of increased gaseous flow rate through the spray nozzle due to the pressure increase is considered in the results.

aerosol transport to be hindered in the setup when there is no spray operation. In addition, the gas flow was immediately diluted at the outlet of CSS, thus decreasing the particle and gaseous species concentrations and lowering the water vapour pressure/avoiding condensation in the gas flow during spray operation. These actions improved the transport of particles and gaseous species downstream of the CSS.

Another fact to support the obtained removal efficiency results (shown above) is that practically the same results were obtained using two completely different methods: INAA analysis of filter samples and ELPI online analysis of particles in the gaseous atmosphere (the conditions of MilliQ water spray).

The tellurium retention in the sump of CSS was also analysed using ICP-MS. However, the results could not be interpreted in a straightforward manner. The amount of tellurium in the sump decreased when the amount of chemicals in the spray droplets was increased. This is the opposite of the observed tellurium removal efficiency. In addition, no visible deposits were observed in the line between the CSS and the filter. Therefore, it was concluded that the analysis of sump samples was not successful, or the sump samples were not representative for the whole sump.

The mass balance of caesium and iodine was rather good, but it deteriorated with the increasing temperature and likely formation of CsOH and gaseous iodine, which could not be accurately analysed. The likely formation of gaseous iodine also led to a loss of iodine due its volatile nature during the storage period before the analysis.

The oxidation of precursor was suggested in some of the experiments and further analysis of the remaining precursor after the experiments was performed using the X-ray diffraction analysis method, see the Supplementary file S1. The XRD analysis verified the partial oxidation of metallic tellurium precursor in Experiments 4 to 9. The fraction of tellurium oxidized in the experiments was also estimated.

5. Results of MELCOR modelling

Experiment 1 with MilliQ water spray solution was modelled using MELCOR code version 2.2. The AMMD of the particles was set to 0.45 µm and the standard deviation was set to 1.41. Based on the MELCOR calculation, 95.7% of the particles were removed by the spray. The measured value was 82.5%. Thus, the MELCOR model significantly overestimated the efficiency of the spray.

The effect of various parameters in the MELCOR model was tested. The AMMD of the particles was 0.45 µm in the base case. Variations between 0.3 µm and 1 µm did not have any significant effect on the calculation result.

On the contrary, the spray droplet size turned out to be an important parameter. In the base case calculation, the droplet size was set to 18 µm, which is the Sauter mean diameter, according to the spray nozzle specifications. The peak of the droplet number distribution is at 10 µm. When the droplet size was decreased from 18 µm to 10 µm, the calculated removal efficiency increased from 95.7% to 99.2%. When the droplet size was increased to 27 µm, the calculated removal efficiency became equal to the measured value (82.5%). This size is near the upper end of the droplet number distribution of the nozzle. In terms of the droplet volume distribution, about 70% of the water volume is in droplets that are smaller than 27 µm.

Considering the change of carrier gas from air to nitrogen, dry to humid and the feed of CsI particles in the other experiments, the MELCOR calculation results did not differ from Experiment 1 significantly. In addition, MELCOR does not consider any difference between Te or TeO$_2$ species and thus, they are handled similarly in the calculations.

6. Discussion and conclusions

The objective in this work was to perform an experimental and modelling study on the removal efficiency of the containment spray system against tellurium species formed under severe accident conditions. As many of the radioactive tellurium isotopes decay into iodine isotopes, which cause a major health risk to the population in case of source term to the environment, the mitigation of tellurium releases inside the containment building would be beneficial.

In the experiments, tellurium was vaporized in the forms of tellurium dioxide and metallic tellurium powders in oxidizing and inert atmospheres, which were either dry, humid or humid with additional CsI particles. The formed tellurium species were exposed to spray droplets composed of MilliQ water, H$_3$BO$_3$-NaOH solution or H$_3$BO$_3$-NaOH-Na$_2$S$_2$O$_3$ solution inside a model containment spray system setup at 20 °C and atmospheric pressure.

Based on the INAA analysis of the collected tellurium particles on filter, the removal efficiency for TeO$_2$ and Te aerosols was above 80% using water spray droplets in the air atmosphere. The chemical spray droplets increased the efficiency above 95%. The further addition of chemicals improved the efficiency somewhat. The removal efficiency for Te aerosol decreased to 55 to 75% in the nitrogen atmosphere. This significant drop in the removal efficiency, which may be due to lower efficiency of Te vapour oxidation in humid N$_2$ atmospheres, should be further investigated. In all atmospheres, the additional airborne CsI particles increased the removal efficiency. The phenomenon was significant in the air atmosphere using water droplets, but it was less pronounced in the case of chemical droplets, which were likely already increasing the removal efficiency. The metallic tellurium removal efficiency in the nitrogen atmosphere increased from 55 to 75% to 90–95% due to the CsI particles. The removal efficiency remained high regardless of the chemical composition of spray droplets. It indicated that the possibility of a chemical reaction between Te and CsI should be considered. The SEM analysis indicated the formation of large crystals in this condition, further coagulating with tellurium aerosol and thus improving the removal efficiency. Based on the TEM/EDX analysis, the crystals were composed of tellurium and oxygen in this condition. The Cs and I could not be detected. The possible peaks of Cs and I were overlapped by the strong peaks of tellurium being the major component in the EDX spectrum. The obtained results for the removal efficiency using water spray droplets were verified based on the ELPI online aerosol analysis data. It was also observed that the chemical spray droplets were forming a significant amount of aerosol particles, which possibly act as seed particles transporting tellurium (and other fission products) further in the containment building; this role should be considered. Another issue was that the formed particles were also interfering with the ELPI measurement because it was overlapping with the tellurium data. The fraction of gaseous tellurium species was too low to make any conclusions on the removal efficiency.

The removal efficiency for Cs and I seemed to reach up to ca. 85% in the form of CsI particles. When the CsI decomposed at higher temperatures, the removal efficiency of both elements decreased due to the likely formation of CsOH and gaseous iodine, which could not be accurately analysed.

The MELCOR code significantly overestimated the particle removal efficiency when the spray droplet size was set to the Sauter mean diameter of the size distribution (18 µm). The calculation result was sensitive to the droplet size. The spray model in MELCOR has been validated with the CSE A9 experiment, in which the droplet size was 1220 µm (Humphries et al. 2015). The droplets in the current experiments were much smaller than those

that are typically representing most of the spray droplets' size distribution used in nuclear power plants and clearly outside the validity range of the MELCOR code.

Overall, it is difficult to differentiate the improvement in the removal efficiency of the investigated tellurium aerosols due to the chemical effect of spray droplets. The major phenomena having an impact on the removal efficiency are likely physical, such as interception, collision, coagulation and adsorption of tellurium with the spray droplets and their dry residuals. On the other hand, after being trapped by the spray droplets, tellurium aerosols may also have chemical reactions within the droplets, which will further improve the removal of tellurium from the containment building atmosphere.

Considering the upscaling to a real reactor scenario, the importance of a containment building atmosphere (oxidizing, inert, dry, humid) on the fission product removal by the CSS was indicated. The airborne fission product and structural aerosols may play a role in the removal efficiency of other species by CSS; caesium iodide particles seemed to enhance the tellurium removal efficiency in this work. On the other hand, the chemical spray droplets may form solid aerosol particles, which may also act as a carrier for other species further in the containment building. These findings complement the existing data on the tellurium behavior in the containment building and the removal of airborne tellurium by the CSS. A major difference to the real reactor scenario is the rather small diameter of the spray droplets used in this work. However, the small droplets are representative for the lower range of the real spray droplet size distribution. The obtained data serves as comparison data against computer models derived based on the large droplet tests. The dependence of tellurium removal efficiency on the surrounding atmospheric conditions indicated in this work contributes to the assessment of tellurium source term and severe accident management actions.

CRediT authorship contribution statement

Teemu Kärkelä: Investigation, Methodology, Formal analysis, Conceptualization, Writing – original draft, Writing - review & editing, Funding acquisition. **Anna-Elina Pasi:** Investigation, Methodology, Formal analysis, Writing – original draft, Writing - review & editing. **Fredrik Espegren:** Investigation, Methodology, Formal analysis, Writing – original draft, Writing - review & editing. **Tuomo Sevón:** Investigation, Software, Writing – original draft. **Unto Tapper:** Investigation, Writing – original draft. **Christian Ekberg:** Funding acquisition, Project administration, Supervision.

Declaration of Competing Interest

The authors declare that they have no known competing financial interests or personal relationships that could have appeared to influence the work reported in this paper.

Acknowledgements

Appendix A. Supplementary data

Aerosol data is available for the mathematical model and code validation purposes, contact: teemu.karkela@vtt.fi. The mass balance and uncertainties in the experiments together with the XRD analysis results of the precursor materials are presented in the Supplementary file S1. Supplementary data to this article can be found online at https://doi.org/10.1016/j.anucene.2021.108622.

References

Ardon-Dryer, K., Huang, Y.-W., Cziczo, D.J., 2015. Laboratory studies of collection efficiency of sub-micrometer aerosol particles by cloud droplets on a single-droplet basis. Atmos. Chem. Phys. 15 (16), 9159–9171.

Ashmore, C.B., Gwyther, J.R., Sims, H.E., 1996. Some effects of pH on inorganic iodine volatility in containment. Nuclear engineering and design 166 (3), 347–355.

Boer, R. de and Cordfunke, E.H.P. (1997). The chemical form of fission product tellurium during reactor accident conditions. J. Nucl. Mater. 240(2), 124 –130. issn: 0022-3115. DOI: 10.1016/S0022-3115(96)00600-9.

Bishop, W.N., Nitti, D.A., 1971. Stability of Thiosulfate Spray Solutions. Nuclear Technology 10 (4), 449–453.

Dehjourian, M., Rahgoshay, M., Sayareh, R., Jahanfarnia, G., Shirani, A.S. (2016). Effect of Spray System on Fission Product Distribution in Containment During a Severe Accident in a Two-Loop Pressurized Water Reactor. Nucl. Eng. Technol. 48(4), pp. 975 –981. ISSN: 1738-5733. DOI: 10.1016/j.net.2016.03.007.

Dora, C., Singh, S., Kumar, S., Datusalia, A., Deep, A., 2010. Development and characterization of nanoparticles of glibenclamide by solvent displacement method. Acta Poloniae Pharmaceutica - Drug Research 67 (3), 283–290.

Espegren, F., Kärkelä, T., Pasi, A.E., Tapper, U., Kučera, J., Lerum, V.L., Omtvedt, J.P., Ekberg, C. (2020). Tellurium Transport in the RCS under conditions relevant for severe nuclear accidents. Submitted to Annals of Nuclear Energy.

Hilliard, R.K., Postma, A.K., McCormack, J.D., Coleman, L.F., 1971. Removal of Iodine and Particles by Sprays in the Containment Systems Experiment. Nuclear Technology 10 (4), 499–519.

Hilliard, R.K., Postma, A.K., 1981. Large-scale fission product containment tests. Nuclear Technology 53 (2), 163–175.

Hinds, W.C. (1999). Aerosol Technology: Properties, Behavior, and Measurement of AirborneParticles. 2nd ed. New York: Wiley, 1999. ISBN: 0471194107

Humphries, L.L., Louie, D. L.Y., Figueroa, V. G., Young, M. F., Weber, S., Ross, K., Phillips, J., Jun, R. J. (2015). MELCOR Assessment Problems, version 2.1.7347. Sandia National Laboratories (SAND2015-6693 R).

Humphries, L.L., Phillips, J., Schmidt, R., Beeny, B., Wagner, K.C., Louie, D. (2019). MELCOR Computer Code Manuals, version 2.2.14959. Sandia National Laboratories (SAND2019-12536 O).

Jones, A.V., Zeyen, R., Sangiorgi, M. (2015). Circuit and Containment Aspects of PHÉBUS Experiment FPT0 and FPT1. Luxembourg: Publications Office of the European Union. EUR 27218. ISSN 1831-9424 (online), DOI: 10.2790/740439

Kissane, M.P., 2008. On the nature of aerosols produced during a severe accident of a water-cooled nuclear reactor. Nuclear Engineering and Design 238 (10), 2792–2800.

Kučera, J., Pasi, A.E., Espegren, F., Kärkelä, T., Lerum, H.V., Omtvedt, J.P., Ekberg, C. (2020). Tellurium determination by three modes of instrumental neutron activation analysis in aerosol filters and trap solutions for the simulation of a severe nuclear accident. Microchem. J. 58, p. 105139. ISSN: 0026-265X. DOI: 10.1016/j.microc.2020.105139.

Laurie, M., March, P., Simondi-Teisseire, B., Payot, F. (2013). Containment behaviour in Phébus FP. Ann. Nucl. Energy 60 (2013), pp. 15 –27. ISSN: 0306-4549. DOI: 10.1016/j.anucene.2013.03.032.

Lavonen, T. (2014). Chemical effects in the sump water pool during post-LOCA conditions: literature review. Lappeenranta University of Technology: Department of Information Technology. Research report. Project code: 81524/FISKES2013. Finland: VTT Technical Research Centre of Finland.

McFarlane, J. (1996). Fission product tellurium chemistry from fuel to containment. In: Proceedings of the Fourth CSNI Workshop on the Chemistry of Iodine in Reactor Safety. (PSI-97-02). Guentay, S. (Ed.). Switzerland, pp. 563–585.

Neeb, K.H., 2011. The radiochemistry of nuclear power plants with light water reactors. Walter de Gruyter.

OECD/NEA (2009). State of the art report on nuclear aerosols. NEA/CSNI/R(2009)5.

Parsly, L.F., 1971. Spray Program at the Nuclear Safety Pilot Plant. Nuclear Technology 10 (4), 472–485.

Pasi, A.-E., Glänneskog, H., Foreman, M.-J., Ekberg, C., 2020. Tellurium Behavior in the Containment Sump: Dissolution, Redox, and Radiolysis Effects. Nuclear Technology 207 (2), 217–227.

Pontillon Y., Ducros G. (2010). Behaviour of fission products under severe PWR accident conditions: The VERCORS experimental programme - Part 2: Release and transport of fission gases and volatile fission products. Nucl. Eng. Design,

Vol. 240, iss. 7, pp. 1853-1866, ISSN 0029-5493, DOI: 10.1016/j.nucengdes.2009.06.024.

Powers, D.A., Burson, S.B. (1993). A Simplified Model of Aerosol Removal by Containment Sprays. NUREG/CR-5966, SAND92-2689.

Sangiorgi, M., Grah, A., Ammirabile, L. (2015). Circuit and Containment Aspects of PHÉBUS Experiment FPT-2. Luxembourg: Publications Office of the European Union. EUR 27631. ISSN 1831-9424 (online), DOI: 10.2790/94418 (online)

Sehgal, B.R., 2011. Nuclear safety in light water reactors: severe accident phenomenology. Academic Press.

Steinhauser, Georg, Brandl, Alexander, Johnson, Thomas E., 2014. Comparison of the Chernobyl and Fukushima nuclear accidents: a review of the environmental impacts. Sci. Total Environ. 470-471, 800–817.

Unscear, 2008. SOURCES AND EFFECTS OF IONIZING RADIATION (annex D). United Nations, New York.